FRACTURE ANALYSIS OF WOOD STRUCTURES USING A MULTI-REGION ANISOTROPIC BOUNDARY ELEMENT FORMULATION

Sérgio Gustavo Ferreira Cordeiro

Edson Denner Leonel

sergio.cordeiro@usp.br

edleonel@sc.usp.br

University of São Paulo, School of Engineering of São Carlos, Department of Structural Engineering.

Av. Trabalhador São Carlense, 400, Centro, 13.566-590 São Carlos-SP, Brazil.

Abstract. *The modelling of crack growth phenomenon in wood using nonlinear fracture approaches has received wide attention by the scientific community in recent years. Among the available techniques for this purpose, the cohesive model has demonstrated to be accurate enough for dealing with the softening behaviour observed during the wood fracture. In addition to that, the Boundary Element Method (BEM) is recognized as accurate and efficient numerical technique capable to address fracture mechanic analyses. Moreover, using the Cruse & Swedlow fundamental solutions, BEM integral equations account the wood anisotropic mechanical response accurately. In this regard, the present study aims at coupling the cohesive crack model with a multi-region anisotropic BEM formulation to simulate the mechanical behaviour of wood specimens subjected to fracture tests. The coupling procedure consists in modelling cohesive cracks along the interfaces of multi-region domains. The nonlinear problem is solved using classical Newton approach, in which try and correction steps are required. Two mode I fracture tests of wood specimens were proposed to validate the presented formulation. The numerical results achieved were compared with experimental and numerical responses available in literature in order to prove the approach accuracy.*

Keywords: *Wood fracture, Anisotropic boundary element method, Cohesive crack model*

1 INTRODUCTION

Wood is a material mechanically efficient in terms of strength/weight ratio if compared to other construction materials. Moreover, wood is capable to resist to a wide range of environmental effects (Smith et al., 2003). Therefore, among the classical engineering materials, wood is commonly used in structures such as bridges, trusses, silos, beams by glued laminated timber and boards. However, the heterogeneity is an inherent trait of the woods. Due to the natural development of the trees, longitudinal fibres along the trunk axe are observed in the wood morphology. Therefore, elastic properties are dramatically dependent on the orientation of the wood natural axes (Bodig & Goodman, 1973). Normally, wood at the macro-scale may be classified as a nonhomogeneous material with a complex morphology that is generally orthotropic (Bodig & Jayne, 1982).

Furthermore, based on experimental observation, it was verified that the interfaces between the longitudinal fibres are considerably weaker than the strength of it cell walls (Jayne, 1960). Therefore, such interfaces can be considered as plans of material weakness were the fracture occurs. Furthermore, woods morphology naturally presents structural defects such as knots, pores and cracks that are observed in a very large range of scales. Such defects coupled to the heterogeneity itself make the material modelling using homogenization procedures and continuum mechanics a hard task for wood structures. Due to the defects and the fragility of the longitudinal fibres interfaces, fracture is the most common failure mode observed in wood structures (Smith et al. 2003). Therefore, many efforts were made in the sense of applying fracture mechanic theory to describe the failure of wood components (Triboulot et al. 1984; Prokopski, 1993; Dourado et. al., 2008; Moura et al., 2010; Coureau et al., 2013; Fakoor & Rafiee, 2013).

In the first studies of this subject, the concepts of Linear Elastic Fracture Mechanics (LEFM) were applied (Atack et al., 1961; Porter, 1964; Schniewind & Pozniak, 1971). However, experimental results indicated a size dependence of the fracture toughness (Barret, 1974; Barret et al., 1995). According to the LEFM concepts, such parameter should be a material property, which do not depend on the specimen dimensions. Such size dependence indicates the presence of a Fracture Process Zone (FPZ), which dissipates energy during the fracture. Therefore, the concepts of Nonlinear Fracture Mechanics (NLFM) started to be applied to wood. According to Smith et al. (2003), Bostrom (1992) was the first to apply a nonlinear fracture model to wood. Based on the well-known cohesive crack model (Hillerborg et. al., 1976), the author proposed a model to describe the wood softening behaviour with a bilinear cohesive law. Ever since, may other authors have also successfully applied the cohesive crack model to describe wood fracture (Moura *et al.*, 2010; Dourado *et al.*, 2011; Coureau et al., 2013).

In this regard, this paper addresses the mechanical analysis of fracture tests performed in wood specimens using a nonlinear Boundary Element Method (BEM) formulation. The BEM is a robust numerical technique for modelling crack problems, as only boundary surfaces discretization is required. In addition to that, this numerical technique is capable to represent accurately the stress concentration at the crack tip. Therefore, BEM is well adapted to solve fracture mechanics problems as pointed out by Portela et al. (1992); Yan (2007) and Leonel & Venturini (2011). To account the wood orthotropic behaviour, a general anisotropic fundamental solutions based on Lekhnitskii formalism was adopted (Cruse & Swedlow, 1971). The BEM formulation involves the multi-region technique coupled to the cohesive crack model. This technique divides the entire domain into sub-regions in which traction equilibrium must be enforced along the interfaces. However, in crack problems, displacement compatibility is no longer verified. Therefore, the cohesive laws are required to relate displacement discontinuities with the tractions at crack surfaces. As a result, cracks in the present work are assumed to growth along sub-region interfaces. One advantage of this approach concerns the possibility to analyse crack propagation in nonhomogeneous materials (Benedetti & Aliabadi, 2013). It is important to mention that the modelling of crack growth in wood structures using BEM has not been observed in literature, which justifies the development of the present research.

Two applications of mode I fracture were performed with the developed formulation and the results were compared with experimental and numerical responses available in literature to prove its robustness and accuracy.

2 BEM INTEGRAL EQUATIONS FOR ANISOTROPIC MEDIA

The BEM has been widely applied in engineering fields such as contact, fatigue and fracture mechanics due to its high accuracy and robustness in modelling strong stress concentration. However, in most of these applications, fundamental solutions for isotropic media are applied. Consequently, the mechanical analyses are limited to problems composed only by some specific materials.

The present study aims to evaluate the wood fracture accounting the wood anisotropic mechanical behaviour. For this purpose, fundamental solutions for anisotropic materials are required. In the present study, the Cruse & Swedlow fundamental solutions are applied.

Considering a two-dimensional homogeneous elastic body with boundary Γ, the singular integral equation, which governs the elastostatic problems, can be presented in Equation (1), disregarding domain forces.

$$c_{ij}(s,f)u_j(s)+\int_\Gamma P_{ij}^*(s,f)u_j(f)\,d\Gamma=\int_\Gamma U_{ij}^*(s,f)\,p_j(f)\,d\Gamma . \tag{1}$$

where p_i and u_i are respectively tractions and displacements on the boundary, c_{ij} is the free term of the singular integrations, which is equal to $\delta_{ij}/2$ for smooth boundaries. P_{ij}^* and U_{ij}^* are the fundamental solutions of tractions and displacements written for the source point s. For general anisotropic solids, such solutions were developed by Cruse & Swedlow (1971) and can be shortly presented as follows.

$$U_{ij}^*(s,f)=U_{ij}^*\left(z_k^0,z_k\right)=2\,\mathrm{Re}\left[q_{i1}A_{j1}\ln\left(z_1-z_1^0\right)+q_{i2}A_{j2}\ln\left(z_2-z_2^0\right)\right] \tag{2}$$

$$P_{ij}^*(s,f)=P_{ij}^*\left(z_k^0,z_k\right)=2\,\mathrm{Re}\left[\frac{1}{\left(z_1-z_1^0\right)}g_{j1}\left(\mu_1\eta_x-\eta_y\right)A_{i1}+\frac{1}{\left(z_2-z_2^0\right)}g_{j2}\left(\mu_2\eta_x-\eta_y\right)A_{i2}\right] \tag{3}$$

where $\mathrm{Re}[\ ]$ represents the real part of a general complex expression. μ_1 and μ_2 are complex roots of the characteristic equation required to obtain the complex stress function that solves the anisotropic elasticity problems (Cruse & Swedlow, 1971). As showed in Lekhnitskii (1963), such equation have four roots, which can be either complex or purely imaginary, two of them being the conjugate of the other two. For instance μ_1, μ_2 are the roots with the imaginary part greater than zero and $\bar{\mu}_1$, $\bar{\mu}_2$ their conjugate. Once these roots depends only on the flexibility matrix, it can be considered as material parameters related with the anisotropy. Furthermore, z_1 and z_2 represent the coordinates of the field points in the domain of the anisotropic solid written for in the two complex spaces as follows in Equation (4).

$$z_k = x + \mu_k y \qquad (k = 1,2) \tag{4}$$

Besides, z_1^0 and z_2^0 are the coordinates of the source point (x_0, y_0) at the complex spaces. η_x and η_y are the cartesian components of the outward normal at the field points and q_{ij} and g_{ij} are constant material properties which can be defined for plane stress as presented in Equations (5) and (6).

$$q_{ij} = \begin{bmatrix} a_{11}\mu_i^2 + a_{12} - a_{16}u_i \\ a_{12}\mu_i + a_{22}/\mu_i - a_{26} \end{bmatrix} \tag{5}$$

$$g_{ij} = \begin{bmatrix} \mu_1 & \mu_2 \\ -1 & -1 \end{bmatrix} \tag{6}$$

The constants a_{ij} are the compliance components of the flexibility matrix. Furthermore, the coefficient A_{ij} are also constant material properties that are obtained from the requirements of unit loads at the source point z_k^0 and from the displacement continuity for the fundamental solution. Their values are obtained from the solutions of the following complex system.

$$\begin{bmatrix} 1 & -1 & 1 & -1 \\ \mu_1 & -\bar{\mu}_1 & \mu_2 & -\bar{\mu}_2 \\ q_{11} & -\bar{q}_{11} & q_{12} & -\bar{q}_{12} \\ q_{21} & -\bar{q}_{21} & q_{22} & -\bar{q}_{22} \end{bmatrix} \begin{Bmatrix} A_{i1} \\ \bar{A}_{i1} \\ A_{i2} \\ \bar{A}_{i2} \end{Bmatrix} = \begin{Bmatrix} \delta_{i2}/2\pi i \\ -\delta_{i1}/2\pi i \\ 0 \\ 0 \end{Bmatrix} \tag{7}$$

In which $\bar{q}_{ij}$ are computed from Eq. (5) considering the conjugated roots $\bar{\mu}_1$, $\bar{\mu}_2$.

3 WOOD FRACTURE BEHAVIOUR

Due to the complex wood morphology, it is important to mention that the fracture parameters of wood also depend on the fracture orientation. Regarding the material anatomic axes, Longitudinal (L), Radial (R) and Tangential (T), there are six principal crack orientation of fracture in wood specimens as illustrated in Fig. 1.

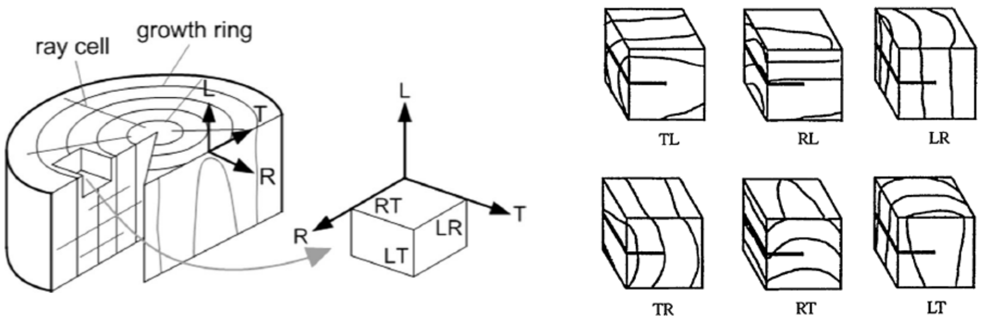

Figure 1. Principal crack orientation systems: Benabou & Sun (2014)

Regarding crack orientations TL, RL, LR, TR, RT and LT, the first indices indicates the perpendicular direction with respect to the fracture plan and the second indices the direction of the crack extension. Combining the crack orientations with the possible fracture modes (modes I, II, II and mixed), there are many possibilities for fracture in wood. However, fracture mode I in the RL and TL crack orientations are generally the first focus of study. Such particular interest occurs because propagation along the longitudinal direction, i.e., propagation with stress perpendicular to the fibres, is the most probable fracture observed in woods. In these conditions, the material weakness plan matches with the plan that maximizes energy release rate.

The concepts of LEFM were firstly applied to describe the wood fracture behaviour. However, a size dependence of the fracture toughness was observed in experimental tests (Schniewind and Pozniak, 1971). This fact indicates the presence of a nonlinear FPZ with considerable dimensions. Nowadays, it is a common sense that experimental wood fracture tests are strongly influenced by nonlinear phenomena (Bostrom, 1992; Tschegg et al., 2001; Smith et al., 2003).

Therefore, NLFM models were proposed for modelling the wood failure. For instance, Bostrom (1992) was the first author to propose a nonlinear fracture model to describe the wood softening behaviour. The nonlinear model adopted was the cohesive crack model from Hillerborg et al. (1976). Such model was successfully applied to describe the softening behaviour in others quasi-brittle materials, such as the concrete and cement based composites (Hillerborg, 1980; Elfgren, 1989). With this approach, the nonlinear FPZ ahead the crack tip is modelled by a fictitious crack with cohesive stresses into its surfaces to represent the residual material strength (Fig. 2b). Therefore, the energy dissipated during the fracture is assumed to occur along the fictitious crack, thus reducing the dissipation zone to a one dimension line. The material degradation is approximated by simple softening laws, which are assumed to govern the residual resistance of the materials along the fictitious crack. These laws relate the crack opening displacement Δu to the cohesive tensile stresses σ_t acting at the fictitious crack surfaces. The model can be illustrated by a uniaxial tensile test as presented in Fig 2a.

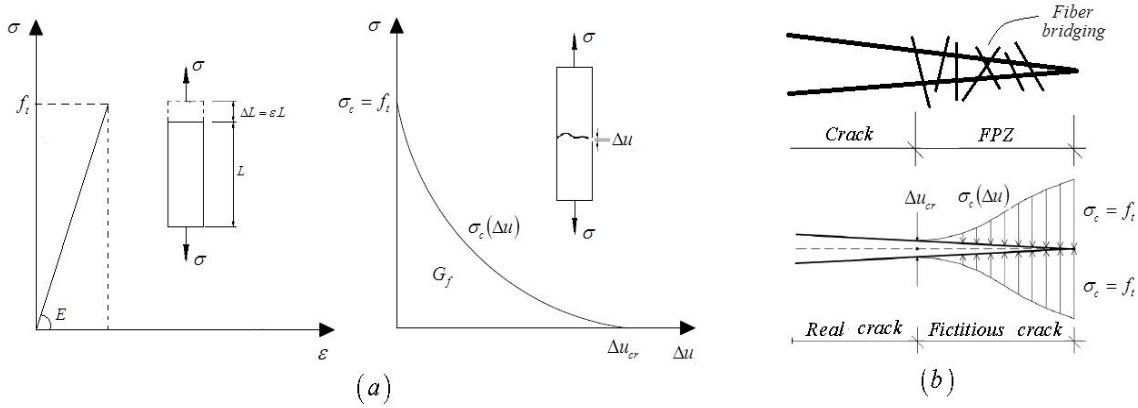

Figure 2. (a) Cohesive crack model (b) cohesive model describing the "fiber bridging" effect

As illustrated in Fig 2, the total energy dissipated during the fracture phenomenon must be equal to the area G_f below the cohesive curve (Fig. 2a). Based on experimental observation, Bostrom (1992) and Stanzl-Tschegg et al. (1995) verified that, among the material dissipating mechanisms, two are the most significant ones: transversal fibres bridging across the crack surfaces and microcracks ahead the crack tip. For instance, fibres bridging can be observed in Fig. 3 in a small scale.

Figure 3. Fibre bridging mechanisms at the FPZ of wood: Vasic & Smith (2002)

In order to represent these fracture nonlinear mechanisms, both authors proposed bilinear cohesive laws as illustrated in Fig. 4.

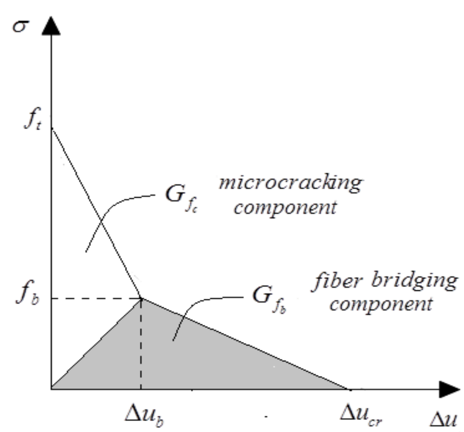

Figure 4. Bilinear cohesive model for parallel to the grain wood fracture

Therefore, for each wood species, the parameters f_t, Δu_{cr}, f_b and Δu_b must be obtained with inverse analysis from the experimental fracture tests.

4 ALGEBRAIC EQUATIONS FOR COHESIVE MULTI-REGION FRACTURE

One possible approach for modelling crack geometries is by the multi-region BEM technique. In this approach, the crack surfaces are discretized by oppositely oriented elements, which compose the interfaces of a given multi-region domain. To analyse the wood fracture, the cohesive crack model was incorporated into these interface elements introducing the nonlinear mechanical behaviour.

Considering multi-region domains, the classical set of algebraic BEM equations is written accounting the location of the collocation points, i.e. source points. These points may be located at the interface opposite elements at left (L) or right (R) sides or even at the boundary (b) of the problem. Hence, the BEM set of algebraic equations can be presented as follows.

$$H_b{}^b u_b + H_b{}^L u_L + H_b{}^R u_R = G_b{}^b p_b + G_b{}^L p_L + G_b{}^R p_R \tag{8}$$

Regarding the cohesive approach, the tractions at the interface-cracked elements depends on the displacement discontinuity. Such discontinuity can be decomposed into the normal and tangential components with respect to the interface orientation. The normal component is known as the Crack Open Displacement (COD) whereas the tangential one is known as the Crack Slide Displacement (CSD). In general, both discontinuity components can dissipate energy. However, for simplicity, it is assumed that only the normal component COD gives rise to energy dissipation during the fracture. Then, the nonlinear model is associated with the normal traction to the crack surfaces and brittle behaviour is assumed for tangential direction. In order to deal with general interfaces orientation, displacements and tractions at the cracked interface must be rotated from x, y global orientation to the normal η and tangent t directions of each crack side as illustrated in Fig. 5.

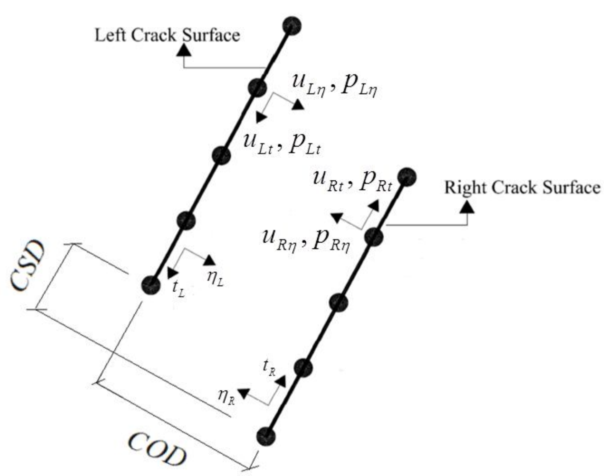

Figure 5. Interface displacements, tractions and discontinuities

where $u_{S\eta}$, u_{St}, $p_{S\eta}$ and p_{St} defines, respectively, the normal (η_S) and tangent (t_S) components of displacements and tractions at a given side $S = L, R$ from an interface. Besides this rotation, it is possible to impose the boundary conditions and then rewrite the Eq. (8).

$$\begin{aligned}&A_b^{\ b}x_b + H_b^{\ L\eta}u_{L\eta} + H_b^{\ Lt}u_{Lt} + H_b^{\ R\eta}u_{R\eta} + H_b^{\ Rt}u_{Rt} = \\ &F_b + G_b^{\ L\eta}p_{L\eta} + G_b^{\ Lt}p_{Lt} + G_b^{\ R\eta}p_{R\eta} + G_b^{\ Rt}p_{Rt}\end{aligned} \tag{9}$$

$H_b^{\ S\eta}, H_b^{\ St}$ and $G_b^{\ S\eta}, G_b^{\ St}$ are composed by the terms that multiply the normal and tangent displacements and tractions. x_b contains the boundary unknown values, $A_b^{\ b}$ is composed by columns of $H_b^{\ b}$ and $G_b^{\ b}$ referent to these values and F_b computes the contribution of the prescribed quantities at the boundary. To solve the multi-region problem it is still required more conditions at the interfaces. For instance, the equilibrium condition for the interface tractions must be imposed.

$$\begin{aligned}&p_{L\eta} = p_{R\eta} = p_\eta \\ &p_{Lt} = p_{Rt} = p_t\end{aligned} \tag{10}$$

Therefore, the algebraic set of equations results.

$$\begin{aligned}&A_b^{\ b}x_b + H_b^{\ L\eta}u_{L\eta} + H_b^{\ Lt}u_{Lt} + H_b^{\ R\eta}u_{R\eta} + H_b^{\ Rt}u_{Rt} = \\ &F_b + \left(G_b^{\ L\eta} + G_b^{\ R\eta}\right)p_\eta + \left(G_b^{\ Lt} + G_b^{\ Rt}\right)p_t\end{aligned} \tag{11}$$

Furthermore, the displacement discontinuities COD and CSD, illustrated in Fig. 3, can now be written in terms of rotated displacement components as follows.

$$\begin{aligned}&-u_{L\eta} - u_{R\eta} = COD \\ &u_{Lt} + u_{Rt} = CSD\end{aligned} \tag{12}$$

Incorporating the relations (12) in Eq. (11), one obtains:

$$\begin{aligned}&A_b^{\ b}x_b + \left(H_b^{\ L\eta} - H_b^{\ R\eta}\right)u_{L\eta} - H_b^{\ R\eta}COD + \left(H_b^{\ Lt} - H_b^{\ Rt}\right)u_{Lt} + H_b^{\ Rt}CSD = \\ &F_b + \left(G_b^{\ L\eta} + G_b^{\ R\eta}\right)p_\eta + \left(G_b^{\ Lt} + G_b^{\ Rt}\right)p_t\end{aligned} \tag{13}$$

Based on the algebraic system of equations presented in Equation (13), it is possible to incorporate the cohesive crack model. Regarding such model, no cracked interface are observed while the normal tractions p_η remains smaller than the material tensile strength f_t. Therefore, $COD = CSD = 0$ and the system of equation becomes linear. However, by imposing the cohesive limit $p_\eta \le f_t$, the elastic solutions obtained for p_η greater then f_t are no longer consistent.

The cohesive model proposes that after such limit the interface stresses must follow a material degradation softening law that can be obtained with inverse analysis from experimental data. The softening behaviour is directly related with energy dissipation. Once it was assumed that only normal stresses could dissipate energy, these softening laws relate the normal tractions p_η with the normal component COD of the discontinuities. Therefore, the normal tractions at the interfaces must follow the cohesive behaviour, which means $p_\eta = p_c(COD)$. Moreover, the tangent tractions f_t must become null after the limit $p_\eta \le f_t$ to complain with the condition of no energy dissipation.

Due to the interdependency of the variables p_η and COD during the fracture analysis, the system of algebraic equations becomes nonlinear. Therefore, an incremental-iterative strategy must be adopted to solve the cohesive problem.

For instance, in a given incremental step, it is always assumed that all the interfaces remains linear elastic. Hence, Eq. (13) can be solved directly with the assumption of null displacement discontinuities. However, at all the interface elements, the normal tractions must be checked, in order to verify if the elastic limit was respected. If in any of the interface collocation points the tractions p_η overcame the tensile strength, nonlinear cohesive behaviour must be imposed at those nodes. Therefore, the set of algebraic equation that must be satisfied should incorporate the cohesive softening laws as follows.

$$\begin{aligned} &A_b^b x_b + \left(H_b^{L\eta} - H_b^{R\eta}\right) u_{L\eta} - H_b^{R\eta} COD + \left(H_b^{Lt} - H_b^{Rt}\right) u_{Lt} + H_b^{Rt} CSD \\ &= \left(G_b^{L\eta} + G_b^{R\eta}\right) p_C\left(COD\right) + F_b \end{aligned} \tag{14}$$

Since the equations are now nonlinear, an iterative strategy must be adopted to correct the solution of the problem in order to satisfy the restriction imposed in Equation (14). The strategy adopted is illustrated in Fig. 6 in which the new equilibrated situation is obtained by the reapplication of the non-equilibrated traction vector.

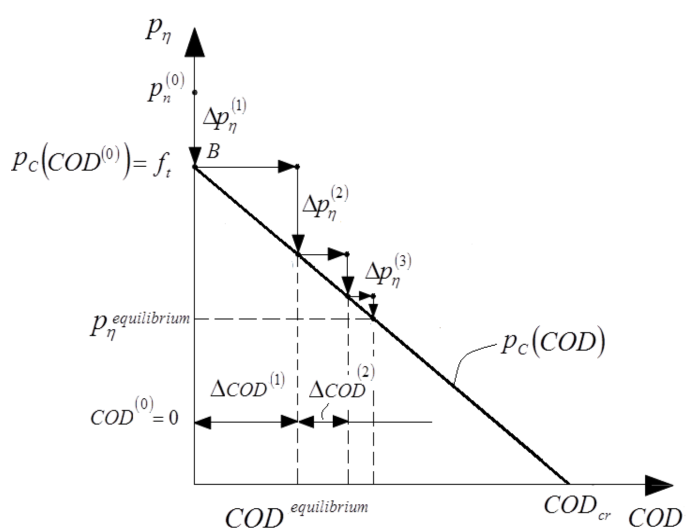

Figure 6. Iterative strategy: Reapplication of over tractions Δp_η

As represented in Fig. 6, when the computed tractions are over the tensile strength f_t (Point A), the over traction $\Delta p_\eta^{(1)}$ must be reapplied into the structure, in the sense of splitting the interface (line AB). Therefore, the contribution of the over traction, $\left(G_b^{L\eta} + G_b^{R\eta}\right)\Delta p_\eta^{(1)}$, must be accounted at the vector of prescribed boundary values F_b. Due to the first correction, the material has no longer the capability for maintaining the interface perfected bonded. Hence, a fictitious opening $\Delta COD^{(1)}$ is computed (line BC). Considering that there is a discontinuity different from zero, the softening cohesive law imposes that the material strength is no longer f_t. Therefore, a second over traction $\Delta p_\eta{}^{(2)}$ is computed and reapplied into the structure (line CD). Again, a new fictitious opening $\Delta COD^{(2)}$ is obtained increasing, hence, the total opening of the interface. This iterative procedure is performed until the over traction $\Delta p_\eta{}^{(i)}$ of a given iteration i become smaller enough to be neglected according to a stop criterion.

The iterative procedure described in Fig. 6 must be performed simultaneously for all the interface nodes in which the normal traction overcame the tensile strength. Therefore, at each iteration i one can group all the over tractions at the cohesive interface points in a vector $\left\{\Delta p_\eta{}^{(i)}\right\}$, which is reapplied at the cohesive interface portion. Hence, the convergence criteria for the iterative procedure may be defined in terms of the norm of this vector. When such scalar norm is smaller than a given tolerance, the incremental nonlinear step converges to the solution.

Normally, the interfaces of a multi-region domain may present three different responses. The first one observed is the Elastic Interface (EI). For this case, no discontinuities are observed for the displacements field. The second response occurs at the Cohesive Interface (CI) portion where the normal tractions are governed by the softening law, $p_\eta = p_C\left(COD\right)$, and the shear tractions p_t becomes null. The last interface behaviour occurs when the normal openings COD overcame a critical value COD_{cr}. When it occurs, the normal tractions also go to zero and the Fractured Interface (FI) becomes a crack free to open and slide. It is important to mention that at the cohesive fracture problems a given interface may present this three distinct behaviour as illustrated in Fig. 7.

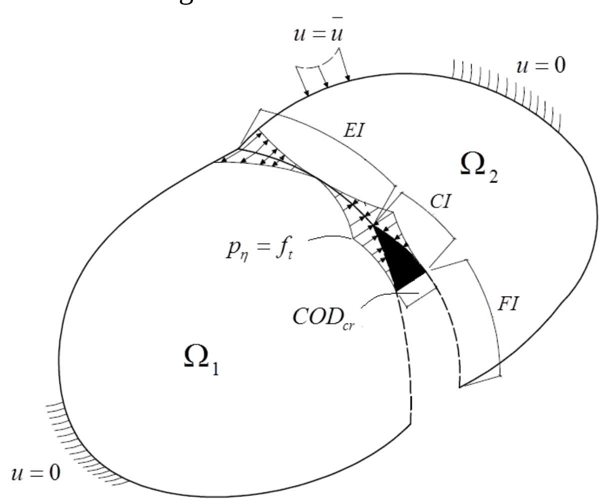

Figure 7. Multi-region interface behaviour: Elastic Interface (EI), Cohesive Interface (CI) and Fractured Interface (FI).

5 APPLICATIONS

Two mode I fracture tests were simulated with the developed BEM formulation. The first one concerns a compact tension specimen test in which the crack is found to be at the RL orientation. The second application addresses a three-point bended beam with a TL crack orientation. Both applications were performed experimentally in previous works with wood specimens.

5.1 Compact tension test in a wood specimen

The first application of this study concerns a compact tension test of a wood specimen performed experimentally and numerically by Bostrom (1992). The wood specie evaluated was the *Pinus Silvestris* and, as the author proposed, a bilinear cohesive law was adopted to represent the fracture degradation process. The cohesive parameters of the law was experimentally determined and were presented as $f_t = 6MPa$, $G_f = 170N/m$, $f_b = 1.05MPa$ and $\Delta u_b = 0.043mm$. The crack was induced to growth in mode I at the direction of the wood longitudinal axis, which is a material weakness plane. Fig. 8 represent the problem and illustrates the elastic orthotropic constant, load conditions and geometrical data written with respect to the longitudinal (L) and radial (R) wood axes.

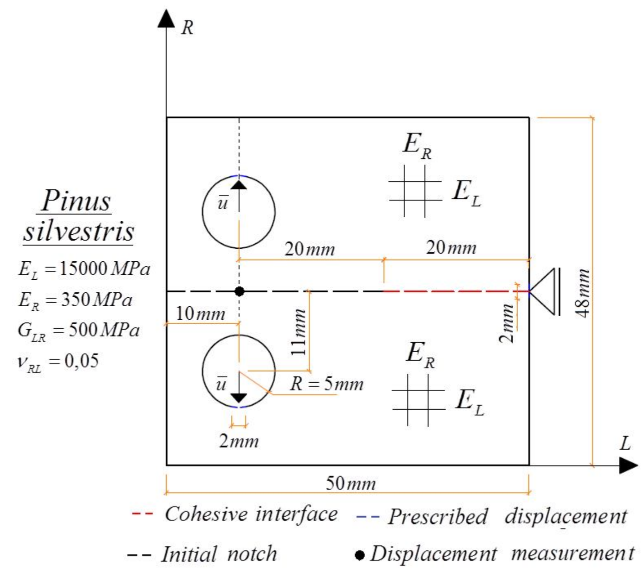

Figure 8. Compact tension test performed in a wood (Pinus Silvestris) specimen

As presented by Bostrom (1992), the thickness of the plate was equal to $20mm$. The adopted boundary mesh consists of 82 quadratic discontinuous elements resulting in 246 collocation points. Prescribed displacements were imposed into 80 increments and the tolerance for the stop criterion was defined as $10^{-6} MPa$. Fig. 9 illustrates the initial and last deformed configuration of the specimen with displacements magnified 10 times.

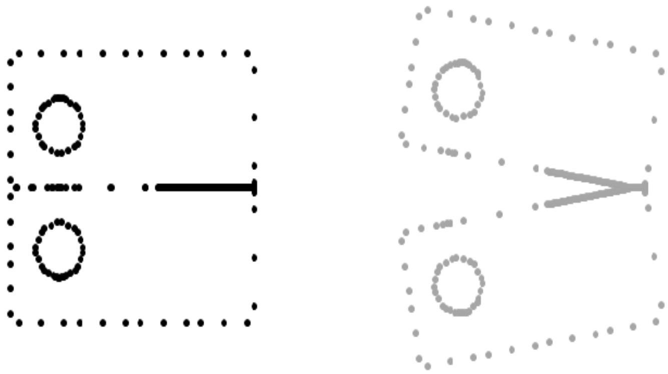

Figure 9. Initial and final deformed meshes. 10 times magnified.

Load-displacement and cohesive stress-COD curves were constructed to compare the structural nonlinear response with the reference ones. The load was considered as the equivalent force at the surface of the superior hole and the displacement was the opening of the initial notch at a measurement point (see Fig. 8). Fig. 10 presents the stress-COD response at the cohesive interface and Fig. 11 illustrates the load-displacement behaviour. The obtained results shows for this application a quite good agreement with the reference responses.

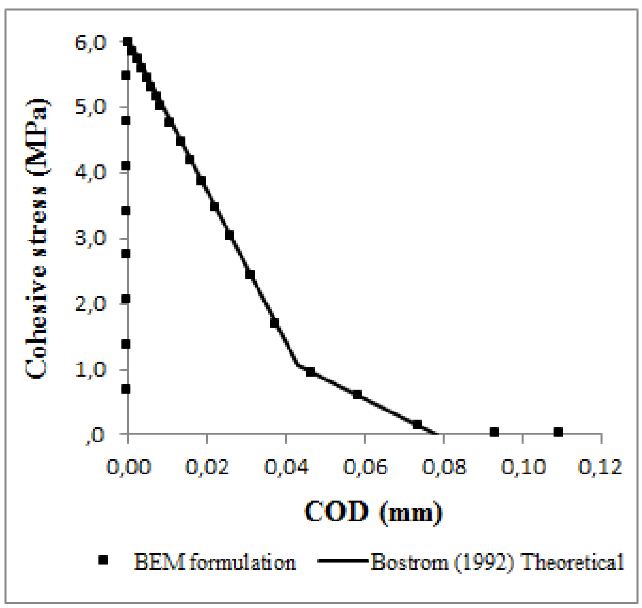

Figure 10. Cohesive stress response: Application 1

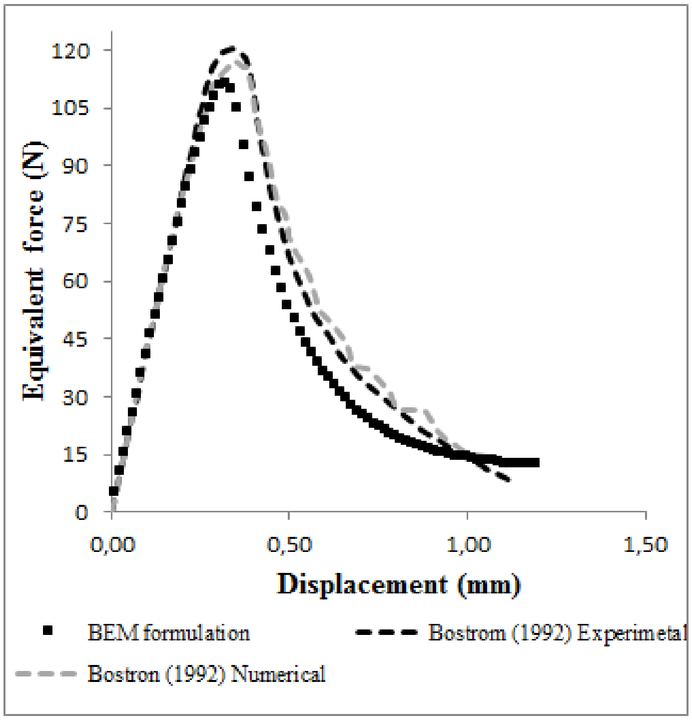

Figure 11. Structure nonlinear response: Application 1

5.2 Three-point bended wood beam

The last application addresses a mode I fracture test of a three-point bended wood beam. The wood specie considered was the Norway Spruce, which was analysed experimentally and numerically by Dourado *et al*. (2008) using a finite element model. The authors proposed another bilinear cohesive law to describe the fracture degradation process of such specie. The cohesive parameters of the law were defined using an inverse analysis of the experimental data. Hence, such properties are: $f_t = 1.66MPa$, $G_f = 144.81N/m$, $f_b = 0.30MPa$ and $\Delta u_b = 0.09mm$. The crack was induced to growth in mode I at a parallel direction of the longitudinal wood fibres (material weakness plane). The specimen was constructed and bonded with a suitable epoxy adhesive in order to comply with the anatomic axes orientation, as represented in Fig. 12. With such scheme, the principal stress near the beam supports do not became parallel to the longitudinal wood fibres, avoiding other cracks to growth besides the main one.

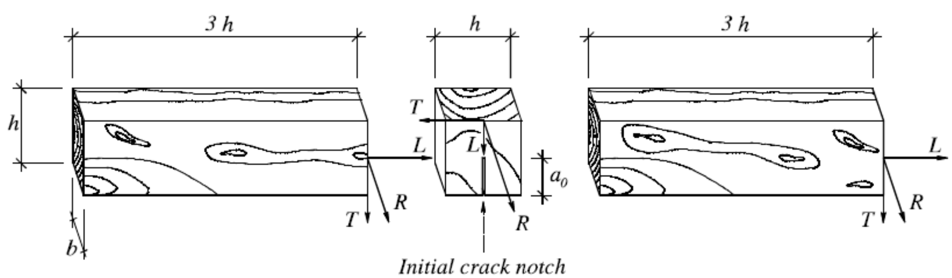

Figure 12. Parts set up before bonding showing the wood axes: (L) longitudinal, (R) radial and (T) tangential (b=40mm, h=70mm, a_0=35mm): Bostrom (1992)

Fig. 13 illustrates the experimental tests performed by Dourado *et al*. (2008) to obtain the softening properties of the wood specie. On the other hand, Fig. 14 presents the geometrical data, load conditions and elastic orthotropic wood constant that were considered to simulate such tests with the numerical BEM technique.

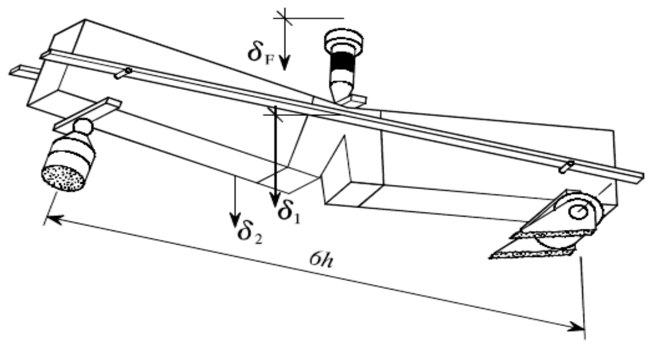

Figure 13. Experimental test scheme (h=70 mm): Dourado et al. (2008)

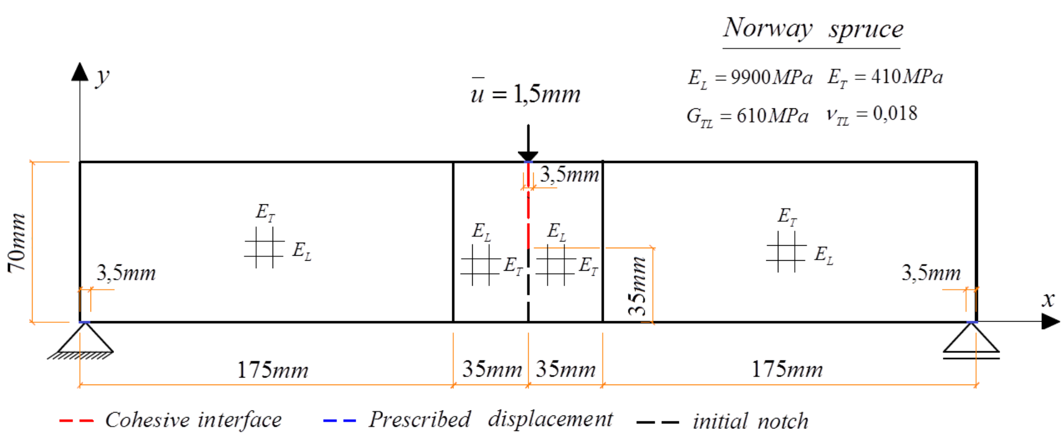

Figure 14. Three-point bended test: Wood (Norway Spruce) beam

The boundary mesh considered was composed by 124 quadratic discontinuous elements resulting in 372 collocation points. The prescribed displacement was imposed into 100 increments and the tolerance for the stop criterion was defined as $10^{-6} MPa$. Fig. 15 illustrates the initial and deformed configuration of the specimen with displacements 30 times magnified.

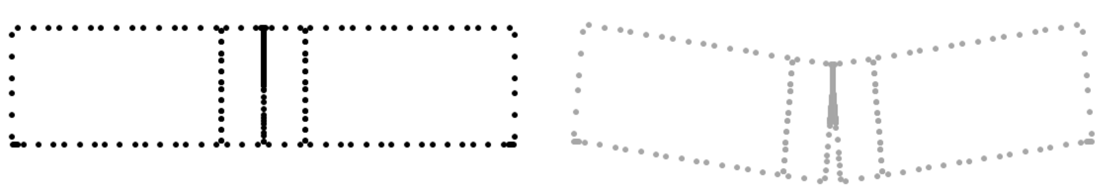

Figure 15. Initial and 30 times magnified deformed mesh

Considering the analysis data, load-displacement and cohesive stress-COD curves were constructed to compare the structural nonlinear response of the specimen with the reference results. The load and displacement were considered as the equivalent force and the vertical displacement at the central point of the superior beam face. Fig. 16 shows the stress-COD behaviour at the cohesive interface whereas Fig. 17 presents the load-displacement response. The results achieved by BEM shows good agreement with the reference, especially in terms of ultimate force.

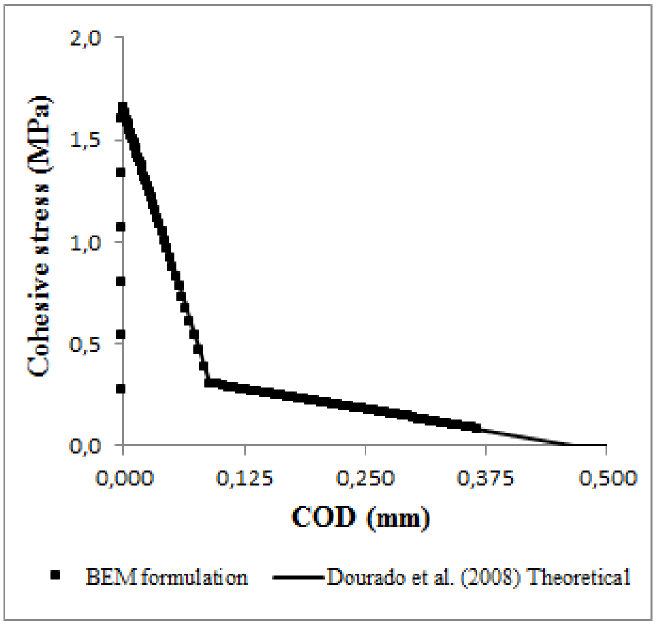

Figure 16. Cohesive stress response: Application 2

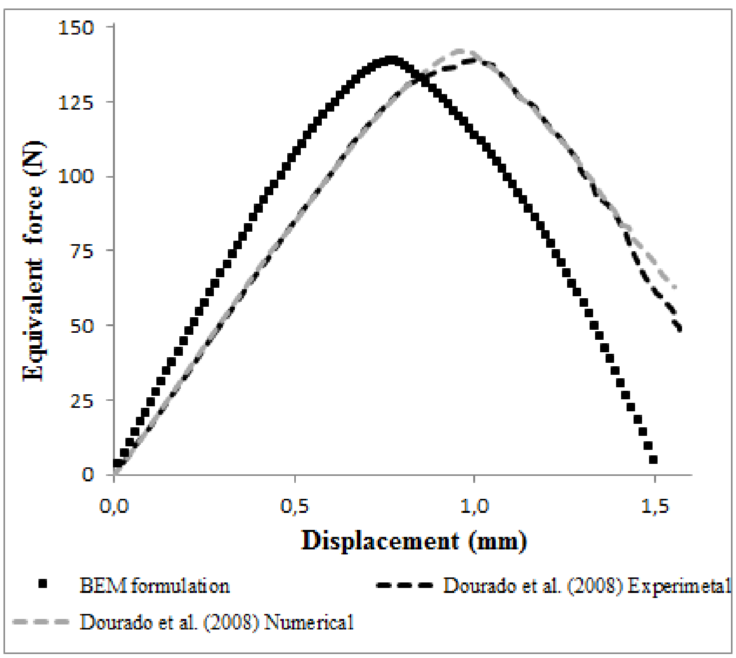

Figure 17. Structure nonlinear response: Application 2

6 CONCLUSIONS

The present study presented a nonlinear BEM formulation to analyse the fracture phenomenon in wood structures. The proposed approach is based on the multi-region technique and the cohesive crack model. As pointed out at the introduction part, this nonlinear fracture model allows the representation of the wood softening behaviour. Furthermore, the use of Cruse & Swedlow fundamental solutions into the BEM integral representations enables the representation of the mechanical anisotropic behaviour observed in wood components.

The presented BEM formulation was applied in two wood specimens, which were experimentally and numerically studied in literature. The results obtained demonstrated the accuracy of the developed BEM formulation in reproducing the nonlinear mechanical response of wood specimens. Such accuracy is emphasized, especially, in terms of ultimate load.

ACKNOWLEDGEMENTS

Sponsorship of this research project by São Paulo Research Foundation (FAPESP), grant number 2014/18928-2 is greatly appreciated. This research is a part of the activities scheduled by the research project USP/COFECUB 2012.1.672.1.0.

REFERENCES

Atack, D., May, W.D., Morris, E.L. & Sproule, R.N., 1961. The energy of tensile and cleavage fracture of black spruce. *Tappi*, vol. 44, n. 8, pp. 555–567.

Barret, J.D ., 1974. Effect of size on tension perpendicular-to-grain strength of douglas-fir. *Wood and Fiber*, vol. 6, pp. 126–143.

Barret, J.D., Lam, F. & Lau, W., 1995. Size effects in visually graded softwood structural lumber. *Journal of Materials in Civil Engineering*, vol. 7, pp. 19–30.

Benabou, L. & Sun, Z., 2014. Numerical study of anisotropic failure in wood under large deformation. *Materials and Structures*, vol. 48, pp. 287–303.

Benedetti, I. & Aliabadi, M.H., 2013. A cohesive boundary element approach to material degradation in three-dimensional polycrystalline aggregates. *Advances in Boundary Element & Meshless Techniques*, vol. 14, pp. 51–55.

Bodig, J. & Goodman, J.R., 1973. Prediction of elastic parameters of wood. *Wood Science*, vol. 5, n. 4, pp. 249–264.

Bodig, J., & Jayne, B.A., 1982. *Mechanics of wood and wood composites*. Van Nostrand Reinhold.

Bostrom, L., 1992. *Method for Determination of the softening behavior of wood and the applicability of a nonlinear fracture mechanics model*. PhD thesis, Lund Institute of Technology/Lund.

Coureau, J.L., Morel, S. & Dourado, N., 2013. Cohesive zone model and quasibrittle failure of wood: A new light on the adapted specimen geometries for fracture test. *Engineering Fracture Mechanics*, vol. 109, pp. 328–340.

Cruse, T.A. & Swedlow, J.L. 1994. *Interactive program for analysis and design problems in advanced composites*. Technical Report AFML-TR-71-268, Carnegie Mellon University.

Dourado, N., Morel, S., de Moura, M.F.S.F., Valentin, G. & Morais, J., 2008. Comparison of fracture properties of two wood species through cohesive crack simulation. *Composites: Part A*, vol. 39, pp. 415–427.

Dourado, N., de Moura, M.F.S.F. & Morais, J., 2011. A numerical study on the SEN-TPB test applied to model I wood fracture characterization. *International Journal of Solids and Structures*, vol. 48, pp. 234–242.

Elfgren, L., 1989. *Fracture Mechanics of Concrete Structures*. Chapman and Hall.

Fakoor, M. & Rafiee, R., 2013. Fracture investigation of wood under mixed mode I/II loading based on the maximum shear stress criterion. *Strength of materials*, vol. 45, n. 3, pp. 378–385.

Hillerborg, A., 1980. Analysis of fracture by means of the fictitious crack model, particularly for fibre reinforced concrete. *International Journal of Cement Composites*, vol. 2, pp. 177–184.

Hillerborg, A., Modeer, M. & Petersson, P-E., 1976. Analysis of crack formation and crack growth in concrete by means of fracture mechanics and finite elements. *Cement and Concrete Research*, vol. 6, pp. 773–782.

Jayne, B.A., 1960. Some mechanical properties of wood fibers in tension. *Forest Products Journal*, June, pp. 316–322.

Leonel, E.D. & Venturini, W.S., 2011. Multiple random crack propagation using a boundary element formulation. *Engineering Fracture Mechanics*, vol. 78, pp. 1077–1090.

Lekhnitskii, S.G., 1963. *Theory of Elasticity of an Anisotropic Body*. Mir Publishers.

Moura, M.F.S.F., Dourado, N. & Morais, J. 2010. Crack equivalent based method applied to wood fracture characterization using the single edge notched-three point bending test. *Engineering Fracture Mechanics*, vol. 77, pp. 510–520.

Moura, M.F.S.F., Oliveira, J.M.Q., Morais, J.J.L. & Xavier, J. 2010. Mixed-mode I/II wood fracture characterization using the mixed-mode bending test. *Engineering Fracture Mechanics*, vol. 77, pp. 144–152.

Portela, A., Aliabadi, M.H. & Rooke, D.P., 1992. Dual boundary element method: effective implementation for crack problems. *International Journal for Numerical Methods in Engineering*, vol. 33, pp. 1269–1287.

Porter, A.W., 1964. On the mechanics of fracture in wood. *Forest Products Journal*, vol. 14, n. 8, pp. 325–331.

Prokopski, G., 1993. The application of fracture mechanics to the testing of wood. *Journal of Materials Science*, vol. 28, pp. 5995–5999.

Schniewind, A.P. & Pozniak, R.A., 1971. On the fracture toughness of Douglas fir wood. *Engineering Fracture Mechanics*, vol. 2, n. 3, pp. 223–233.

Smith, I., Landis, E., & Gong, M., 2003. *Fracture and Fatigue in Wood*. John Wiley & Sons Ltd.

Triboulot, P., Jodin, P. & Pluvinage, G., 1984. Validity of fracture mechanics concepts applied to wood by finite element calculation. *Wood Science and Technology*, vol. 18, pp. 51–58.

Tschegg, E.K., Fruhmann, K. & Stanzl-Tschegg, S.E, 2001. Damage and fracture mechanisms during mode I and III loading of wood. *Holzforschung*, vol. 55, n. 5, pp. 525–533.

Vasic, S. & Smith, I., 2002. Bridging crack model for fracture of spruce. *Engineering Fracture Mechanics*, vol. 69, pp. 745–760.

Yan, X., 2007. Automated simulation of fatigue crack propagation for two-dimensional linear elastic fracture mechanics problems by boundary element method. *Engineering Fracture Mechanics*, vol. 74, pp. 2225–2246.